JBC Papers in Press. Published on February 28, 2005 as Manuscript M501731200

# BORRELIA BURGDORFERI BINDS FIBRONECTIN THROUGH A TANDEM BETA ZIPPER – A COMMON MECHANISM OF FIBRONECTIN BINDING IN STAPHYLOCOCCI, STREPTOCOCCI AND SPIROCHETES.

**Sophie Raibaud[a*], Ulrich Schwarz-Linek[a*], Jung Hwa Kim[b], Huw T. Jenkins[a], Elizabeth R. Baines[a], Sivashankarappa Gurusiddappa[b], Magnus Höök[b] and Jennifer R. Potts[a]**

**From the [a] Department of Biochemistry, University of Oxford, Oxford OX1 3QU**

**[b] Center for Extracellular Matrix Biology, Institute of Biosciences and Technology, Texas A&M University System Health Science Center, Houston, Texas 77030-3303**

Running Title: Fibronectin-binding of *Borrelia burgdorferi*

Address Correspondence to: Jennifer R. Potts, Department of Biochemistry, University of Oxford, South Parks Road, Oxford OX1 3QU Tel: 44 1865 275775, Fax:44 1865 275 253, Email: jennifer.potts@bioch.ox.ac.uk

[*]These authors contributed equally to the work

**BBK32 is a fibronectin-binding protein from the Lyme disease-causing spirochete *Borrelia burgdorferi*. Here it is shown that BBK32 shares sequence similarity with fibronectin module-binding motifs previously identified in proteins from *Streptococcus pyogenes* and *Staphylococcus aureus*. Nuclear magnetic resonance spectroscopy and isothermal titration calorimetry are used to confirm the binding sites of BBK32 peptides within the N-terminal domain of fibronectin and to measure the affinities of the interactions. Comparison of chemical shift perturbations in fibronectin F1 modules on binding of peptides from BBK32, FnBPA from *S. aureus* and SfbI from *S. pyogenes* provides further evidence for a shared mechanism of binding. Despite the different locations of the bacterial attachment sites in BBK32 compared with SfbI from *S. pyogenes* and FnBPA from *S. aureus*, an anti-parallel orientation is observed for binding of the N-terminal domain of fibronectin to each of the pathogens. Thus, these phylogenetically and morphologically distinct bacterial pathogens have similar mechanisms for binding to human fibronectin.**

Lyme borreliosis is the most prevalent and widespread vector-borne human infection in the northern hemisphere (1). The mechanisms through which *Borrelia burgdorferi* colonizes the host are poorly understood, but the pathogen appears to have evolved a number of strategies that allow it to bind to host tissue. The *B. burgdorferi* genome has been completely sequenced (2) and is remarkable for the large number of sequences encoding predicted or known lipoproteins including outer-surface proteins many of which are likely to be involved in interactions with host tissue.

Immunolocalization studies suggest that Fn can bind uniformly over the surface of *B. burgdorferi* (3). Fibronectin (Fn) is a human extracellular glycoprotein involved in important physiological processes such as cell migration and wound healing. Fn is targeted by the pathogenic bacteria *Staphylococcus aureus* and *Streptococcus pyogenes* through bacterial cell-wall attached Fn-binding proteins (FnBPs) (4). These FnBPs belong to a class of adhesins called MSCRAMMS (microbial surface components recognizing adhesive matrix molecules) (4-6). The abilities of FnBPs to mediate adhesion to host tissue and invasion of non-phagocytic host cells (7-9) has generated considerable interest in the structural biology of FnBP/Fn binding. The first high resolution structural data for these interactions (10) revealed a novel mechanism of protein-protein interaction and lead us to propose a new model for binding of *S. pyogenes* and *S. aureus* to the N-terminal domain (NTD) of Fn (10). The NTD of Fn contains five F1 modules ($^{1\text{-}5}$F1) each with a consensus fold containing a double-stranded anti-parallel β-sheet and a triple-stranded anti-parallel β-sheet. In this model, structurally disordered Fn-binding repeats (FnBRs) within the bacterial FnBPs bind $^{1\text{-}5}$F1 or $^{2\text{-}5}$F1 in the NTD of Fn, primarily by forming an additional β-strand on the triple stranded β-sheet of each F1 module. We showed previously that these FnBRs contain strings of F1-binding motifs in the correct order to bind the consecutive F1 modules in the NTD (11). FnBPs from both *S. pyogenes* and *S. aureus* contain multiple FnBRs (10)

BBK32, a 47kDa Fn-binding lipoprotein identified in *B. burgdorferi* (12), is up-regulated under conditions that mimic those encountered by the bacterium during transmission from tick to mammalian host (12) and has also been shown to be

Copyright 2005 by The American Society for Biochemistry and Molecular Biology, Inc.

present during systemic infection in the murine host (13). In humans, BBK32 antigens are observed in infected individuals (14) suggesting that the protein is present during human infection. Antibodies to BBK32 can partially protect mice from tick-borne infection (13).

BBK32 consists of a C-terminal globular domain and an N-terminal region lacking well-defined secondary structure (15). Previously, the Fn-binding activity of BBK32 was localised to a 32 residue peptide within the unstructured domain that shares sequence homology (in the N-terminus of the peptide) to the UR region of an FnBP (SfbI) from *S. pyogenes* (16). This region of SfbI had been shown to bind to the gelatin-binding domain (GBD) of Fn (17) (Fig.1). More recently it was shown that, like the FnBPs from *S. aureus* and *S. pyogenes*, the disordered region of BBK32 undergoes a significant conformational change on binding to the NTD of Fn with an increase in β-sheet content in the complex (15). This suggests that BBK32 could interact with the NTD of Fn in a similar way to the FnBPs of *S. aureus* and *S. pyogenes*. Here we show that BBK32 has sequence similarity to F1-binding motifs within *S. aureus* and *S. pyogenes* FnBPs. Although the similarity is limited, we successfully locate a string of F1-binding motifs in the correct order to bind sequential F1 modules in the NTD of Fn. Comparison of NMR chemical shift perturbations of residues in F1 modules on binding of peptides from BBK32, FnBPA and SfbI provide further evidence for a common mechanism of Fn binding between these pathogens.

## Materials and Methods

*Recombinant Proteins and Synthetic Peptides*– Uniformly (U) $^{15}$N-labeled module pairs $^{2}$F1$^{3}$F1 and $^{4}$F1$^{5}$F1 (residues 62-151 and 152-244 of mature human Fn) were expressed in *Pichia pastoris* and purified using procedures similar to those described previously (10,18). BBKFF, BBKFo, BBKTT, BBKTTb, BBKTw, PyTw5, PyFo5, AuTw1 and AuFo3 were purchased from Alta Bioscience (Birmingham, UK). The N- and C-termini of these synthetic peptides were capped by acetylation and amidation at the N- and C-termini, respectively.

*NMR Spectroscopy*–All NMR experiments were performed on spectrometers belonging to the Oxford Centre for Molecular Sciences with $^{1}$H operating frequencies of 500 and 600 MHz. The spectrometers are all equipped with Oxford Instruments superconducting magnets, OMEGA software and digital control equipment (Bruker Instruments), homebuilt triple-resonance pulsed-field gradient probe-heads (19) and home-built linear amplifiers for $^{1}$H, $^{15}$N and $^{13}$C nuclei. Spectra were recorded at 25°C, processed using the program Felix (Accelrys, San Diego, CA) and analysed using NMRView5.0 (20). $^{1}$H-$^{15}$N Heteronuclear single quantum correlation (HSQC) spectra were acquired of samples of U-$^{15}$N$^{2}$F1$^{3}$F1 or U-$^{15}$N$^{4}$F1$^{5}$F1 with increasing concentrations of peptide. Due to the pH dependence of the solubility of the peptides and Fn module pairs, experiments using BBKTT, BBKTTb and BBKTw were performed at pH 7, experiments using BBKFF and BBKFo were performed at pH6.0, and experiments with AuTw1 and AuFo3 were performed at pH5. For experiments with BBKTT, BBKTw, BBKFF and BBKFo, AuTw1 and AuFo3 the F1 module pair concentration was ~ 0.2mM and for the BBKTTb experiment, the $^{2}$F1$^{3}$F1 concentration was 0.06mM. Module pair concentrations were determined by measuring the absorbance at 280nm. Peptide concentrations were determined using either absorbance at 280nm or the mass. In the NMR titration experiments, peptide concentration was increased until binding was saturated or the solubility limit of the peptide was reached. $^{15}$N-$^{1}$H chemical shift assignments for U-$^{15}$N$^{2}$F1$^{3}$F1 or U-$^{15}$N$^{4}$F1$^{5}$F1 at appropriate pH values were obtained using previously determined assignments (11,21) at pH5.0 and using HSQC spectra acquired at a range of pH values. For assignment of the HSQC of U-$^{15}$N$^{4}$F1$^{5}$F1 when bound to BBKFF, three-dimensional NOESY-HSQC and TOCSY-HSQC spectra of U-$^{15}$N$^{4}$F1$^{5}$F1 (0.5mM)/BBKFF (2.1mM). For all peptides, Fn residues affected by peptide binding were identified on the basis of observed chemical shift changes of F1 module backbone amide resonances (chemical shift perturbation mapping). Dissociation constants ($K_d$s) for the interactions were calculated as previously described (10) using at least eight titrating chemical shifts in each spectrum.

*Isothermal Titration Calorimetry*–The $K_d$ for binding of BBKTTb to $^{2}$F1$^{3}$F1 was measured at 25°C in 10mM sodium/potassium phosphate buffer (pH 7.4) with a VP-ITC microcalorimeter (MicroCal Inc, Northampton, MA). BBKTTb and $^{2}$F1$^{3}$F1 concentrations were determined by measuring the absorbance at 280nm.

Both the cell (containing the $^{2}$F1$^{3}$F1 module pair, 0.22mM) and syringe solutions (containing BBKTTb, 3.07mM) were degassed at 15°C for 20 min. One preliminary injection was 2μl, and 37 injections were of 6μl with a stirring speed of 310 rpm and a delay between injections of 3 min. To take into account heat of dilution, a blank titration

was performed by injecting peptide solution into buffer and the linear prediction of this heat of dilution was subtracted from the main experiment. Data were analyzed using MicroCal Origin software, fitting them to a single binding site model.

## Results

*Prediction of F1-binding peptides from BBK32 using S. pyogenes and S. aureus FnBP sequences*– Fig. 1 shows a sequence alignment of residues 126-190 of BBK32 with FnBRs from *S. pyogenes* and *S. aureus* (10). Sequence homology between the UR (GBD-binding) region of SfbI, an FnBP from *S. pyogenes* and BBK32 was reported previously (16). We recently showed that directly C-terminal of the UR region in SfbI is an NTD-binding region containing five FnBRs. Within these FnBRs, we identified motifs which bind to specific F1 module pairs. Here we use the limited similarity between these F1-binding motifs and the BBK32 sequence, to successfully identify F1-binding motifs of BBK32 in the correct order to bind to sequential F1 modules in the NTD of Fn. Thus, we used Fig. 1 to predict $^{2}$F1$^{3}$F1- (BBKTT, BBKTTb) and $^{2}$F1- (BBKTw) and $^{4}$F1$^{5}$F1- (BBKFF) and $^{4}$F1- (BBKFo) binding peptides from BBK32.

*Binding of BBK32 peptides to $^{4}$F1$^{5}$F1*–Chemical shift perturbations observed for the backbone amide $^{1}$H and $^{15}$N nuclei for residues in $^{4}$F1$^{5}$F1 on addition of BBKFF and BBKFo are shown in Fig. 2. On addition of BBKFF to $^{4}$F1$^{5}$F1, significant chemical shift changes are observed in residues from both $^{4}$F1 and $^{5}$F1. This suggests that both modules are involved in the interaction with BBKFF. On addition of BBKFo (in which the predicted $^{5}$F1-binding motif has been removed; Fig.1) the most significant chemical shift changes are observed for residues in $^{4}$F1, with changes in $^{5}$F1 restricted to residues close to the previously identified interface between the two F1 modules (22). Residues 231 and 232 in the D-E loop and residues 236 and 238 in the E strand of $^{5}$F1 undergo $^{15}$N chemical shift perturbations of > 1ppm on addition of BBKFF, but have only small perturbations on addition of BBKFo to $^{4}$F1$^{5}$F1. In $^{4}$F1, residues 188 and 190 in the D-E loop, residues 191-195 in the E-strand, and a single residue (V180) in strand D undergo the largest chemical shift perturbations on addition of BBKFo. The $K_d$s for binding of BBKFF and BBKFo to $^{4}$F1$^{5}$F1 were determined to be 20±6μM and 590±50μM, respectively. The higher affinity binding of BBKFF is consistent with the binding of this peptide to both $^{4}$F1 and $^{5}$F1 while BBKFo binds only $^{4}$F1. Thus, Fig. 2 demonstrates that BBKFF and BBKFo bind to their predicted targets in the N-terminal domain of Fn. In addition, the chemical shift perturbation data supports an anti-parallel orientation of binding of BBK32 to $^{4}$F1$^{5}$F1 and the importance of the D-E loop and E-strand residues in peptide binding.

*Binding of BBK32 peptides to $^{2}$F1$^{3}$F1*–The sequence alignment in Fig. 1 was used to identify $^{2}$F1 and $^{3}$F1-binding motifs in BBK32. A comparison of chemical shift perturbations of $^{2}$F1$^{3}$F1 resonances on addition of BBKTT (Fig. 3A) and BBKTw (Fig. 3B) clearly shows that both modules in $^{2}$F1$^{3}$F1 are involved in binding to BBKTT whereas BBKTw binds $^{2}$F1. On addition of BBKTw, which lacks the N-terminal (predicted $^{3}$F1-binding) residues, chemical shift changes were observed primarily for residues in $^{2}$F1. In particular, residues 144 in the D-E loop and residues 145 and 146 in the E -strand of $^{3}$F1, which show the largest $^{1}$H chemical shift changes (of $^{3}$F1 residues) on addition of BBKTT, undergo only very small changes on binding of BBKTw. Significant changes in the chemical shift of some $^{3}$F1 residues are observed on addition of the shorter peptide. These residues (for example S117 in strand B) are in strands A and B and in the D-E loop which would be predicted, on the basis of the structure of the homologous $^{4}$F1$^{5}$F1 module pair (22), to form part of an interface between the $^{2}$F1 and $^{3}$F1 modules. The chemical shift perturbation data supports an anti-parallel orientation of binding of BBK32 to $^{2}$F1$^{3}$F1, with the N-terminal part of the peptide binding to the C-terminal module in the pair. In BBKTw, the C-terminus was extended but this clearly has very little effect on the chemical shift changes in $^{2}$F1. This suggested that the C-terminus of BBKTT correctly marked the boundary of the $^{2}$F1-binding motif. The $K_d$'s for the interactions were then compared (Fig. 3D&E). BBKTT bound with a $K_d$ of 230±60μM while BBKTw bound with a $K_d$ of 38±6μM. This was not consistent with our previous comparisons of F1-binding motifs, where the module-*pair* binding peptides bind with higher affinity than the single module binding peptides. Thus the binding of an additional peptide, BBKTTb, which had a shorter N-terminus but longer C-terminus, was tested. By comparison of Fig. 3C and Fig. 3A, it is clear that the main changes in chemical shift perturbation occur in the E-strand of $^{3}$F1, suggesting that part of the $^{3}$F1-binding motif has been removed by truncating the N-terminus of the peptide. The $K_d$ for binding of BBKTTb to $^{2}$F1$^{3}$F1 was 30μM. This almost 10-fold difference between *Kd*s for the interaction of the two (BBKTT and BBKTTb) $^{2}$F1$^{3}$F1-binding peptides with $^{2}$F1$^{3}$F1

suggests that despite the subtle differences in backbone chemical shift perturbations, a residue near the C-terminus of BBKTTb (which was not included in BBKTT) interacts with the sidechain of a $^{2}$F1 residue. This interaction appears to make a significant contribution to the affinity of the interaction and high resolution structural studies are underway to reveal further details of these interactions.

*Comparison of chemical shift perturbation in $^{2}$F1 and $^{4}$F1 on binding of Fn-binding peptides from B. burgdorferi, S. pyogenes and S. aureus*–The successful identification above of Fn-binding BBK32 peptides based on a sequence alignment of BBK32 with FnBPs from *S. pyogenes* and *S. aureus* provides strong evidence for a common mechanism of Fn-binding for these three pathogens. However, further evidence can be obtained by comparing the pattern of chemical shift changes in F1 modules observed on binding of the bacterial peptides. In Fig. 4, the pattern of backbone amide $^{15}$N and $^{1}$H chemical shift perturbations for residues in $^{2}$F1 (A-C) and $^{4}$F1 (D-F) on binding of BBKTw and BBKFo respectively, is compared with the changes observed on binding of $^{2}$F1- and $^{4}$F1-binding motifs from *S. pyogenes* and *S. aureus*. From the concentration of large perturbations in the C-terminal region of both the modules this figure clearly shows the involvement of residues in the D-E loop and E-strand of the F1 module in binding to all six peptides. Also, given the differences in the sequences of the peptides, there are striking similarities in the patterns of these perturbations (highlighted in Fig. 4). Residues in the A-strand also undergo significant chemical shift changes on binding of the six peptides, with the pattern of changes strikingly similar for binding of the $^{4}$F1-binding peptides.

## Discussion

Based on the first high resolution structural data for Fn/bacterial FnBP interactions (10), we recently proposed a model for *S. aureus* and *S. pyogenes* binding to Fn where structurally disordered Fn-binding repeats in the C-terminal region of FnBPs bind to the NTD of Fn primarily by formation of short anti-parallel β-strands on the triple-stranded β-sheet of sequential F1 modules of the NTD (4,10,11). In this tandem β-zipper mechanism of FnBR/Fn binding, we showed that each F1 module is recognised by short motifs within the bacterial FnBRs resulting in the formation of a high affinity binding site for Fn (11).

Previously, the unstructured N-terminal region of BBK32 from the Lyme disease pathogen *B. burgdorferi* was shown to undergo a significant conformational change with an apparent increase in β-sheet content (15) on binding to the NTD of Fn. This was reminiscent of the results of similar experiments performed using a streptococcal FnBP (23) and consistent with BBK32 binding to Fn using the tandem β-zipper mechanism. In addition, BBK32 had been shown to share sequence homology with the GBD-binding region of SfbI from *S. pyogenes* (16). In SfbI from *S. pyogenes*, binding sites for the NTD of Fn lie C-terminal to the GBD binding site. With the hypothesis that this may also be true for BBK32, we used sequence alignments of BBK32 with NTD-binding regions from FnBPs of *S. pyogenes* and *S. aureus* (Fig. 1) and identified potential binding sites within BBK32 (BBKTT and BBKFF; Fig. 1) for modules pairs from the NTD of Fn.

Comparison of chemical shift perturbations on binding of BBK32 peptides to F1 module pairs, shows the involvement of $^{2}$F1, $^{3}$F1, $^{4}$F1 and $^{5}$F1 in the binding to BBK32. As observed previously, for SfbI from *S. pyogenes*, that the orientation of binding of BBK32 to Fn is anti-parallel, that is, the C-terminus of BBKTT (BBKTw) binds $^{2}$F1, and the C-terminus of BBKFF (BBKFo) binds $^{4}$F1. Thus we have identified a sequence of F1-binding motifs in BBK32 in the correct order to bind sequential F1 modules ($^{2\text{-}5}$F1) in the NTD of Fn. The anti-parallel orientation of binding is consistent with the putative GBD-binding sequence lying N-terminal to the NTD-binding sequence (Fig. 5). As in the FnBRs FnBPA-1-11 and SfbI-1-4 from *S. aureus* and *S. pyogenes*, respectively (10), a $^{1}$F1 binding motif has not yet been identified in BBK32.

The chemical shift perturbation data provide important clues to the mechanism of binding. When chemical shift perturbations in $^{2}$F1- and $^{4}$F1- on binding of BBK32 are compared to those observed on binding of *S. aureus* and *S. pyogenes* Fn-binding peptides (Fig. 4), it is clear that all three pathogens bind to the same surface of the F1 modules. The similarity between the magnitude and direction of the largest shifts is striking given the differences between the bacterial peptide sequences. Furthermore, the evidence for the involvement in the binding of the E- strand residues in each of the F1 modules, together with the previous evidence for an increase in β-strand content in BBK32 on binding to Fn (15), provide very strong evidence that BBK32 uses the tandem β-zipper mechanism previously identified for streptococcal binding to Fn (10). Although we have shown that BBK32 contains

$^{2}$F1-, $^{3}$F1-, $^{4}$F1- and $^{5}$F1- binding motifs, and have identified the approximate N-and C-termini of the $^{2-5}$F1-binding sequence, the sequence similarity of BBK32 with FnBPs from Gram-positive bacteria is insufficient for identification of the specific bacterial residues involved in F1 module binding. The length of BBKFF (18 residues) is consistent with the length of previously identified $^{4}$F1$^{5}$F1-binding peptides (PyFF5 - 19 residues) (11). The optimal $^{2}$F1$^{3}$F1-binding peptide, however, appears to be at least 24 residues in length. This is significantly longer than previously identified $^{2}$F1$^{3}$F1-binding peptides from *S. pyogenes* (PyTT5 - 18 residues; PyTT4 - 19 residues) (11), and may justify a different alignment of the sequences in Fig. 1 where, for example, gaps are included between the $^{2}$F1- and $^{3}$F1-binding motifs. Other alignments of the FnBPs (other than that shown in Fig. 1A) with higher similarity in regions of the $^{2}$F1-binding and $^{4}$F1- binding motifs of the Gram positive FnBPs are possible if significant gaps are introduced into these Gram-positive FnBP sequences (Fig. 1B). In addition, sequence similarity cannot be used to identify the 'register' of the anti-parallel β-zipper interaction with the NTD of Fn. That is, to identify which BBK32 and Fn residues are opposed in the β-sheet. Having established this unexpected similarity between the NTD-binding mechanisms of *B. burgdorfer*i and Gram-positive bacteria, we aim obtain to high resolution structural data for BBK32/NTD complexes to answer these questions.

It is shown that, as in *S. pyogenes* binding to Fn, binding of BBK32 to the NTD occurs in an anti-parallel orientation. This is perhaps a little surprising, as the BBK32 membrane attachment site is near the N-terminus while FnBPs of *S. pyogenes* and *S. aureus* are attached to the bacterial cell wall near the C-terminus of the protein. The conservation of the anti-parallel orientation of Fn despite the difference in location of the bacterial attachment site suggests that if the role played by the *S. pyogenes* and *B. burgdorferi* FnBPs is similar, it is independent of the orientation of Fn with respect to the bacterial cell-surface. That is, in SfbI, $^{1}$F1 binds closest (in sequence) to the cell-wall attachment site, while in BBK32, the GBD binding site and then $^{5}$F1 would lie closest to the bacterial surface (Fig. 5). This would be consistent with ours (4) (and others) previous suggestion that bacterial proteins play a role in activating Fn so that the RGD sequence, in the central region of Fn, is accessible for integrin binding (4).

FnBP-mediated uptake of *S. aureus* and *S. pyogenes* may allow these bacteria to evade the host immune system or administered antibiotics, aiding the persistence of the bacteria within the host. We and others have suggested that multiple Fn-binding sites may play a role in integrin-clustering and subsequent uptake of *S. pyogenes* and *S. aureus* into epithelial cells (4). Unlike SfbI from *S. pyogenes* and FnBPA from *S. aureus* which both contain multiple Fn binding sites (11,24), to date only one Fn-binding site has been identified in BBK32. However, integrin clustering might also be achieved through binding of Fn to multiple copies of the FnBP. Whether BBK32 mediates uptake of *B. burgdorferi* into epithelial or endothelial cells *in vivo* has yet to be established although *in vitro* invasion of endothelial cells by *B. burgdorferi* has been reported *(25)*. It has also been shown *in vitro* that *B. burgdorferi* is able to attach to the apical surface of endothelial cells, migrate through the intercellular spaces and into the sub-endothelial matrix. Thus, cellular invasion, which has been suggested to play a role in hematogenous dissemination of *S. aureus* and *S. pyogenes*, may not be necessary for *B. burgdorferi* migration.

The spirochete *B. burgdorferi* is morphologically distinct from the Gram positive pathogens *S. aureus* and *S. pyogenes*. For example, spirochetes are motile, tightly coiled, bacteria 8-30μm in length, whereas *S. aureus and S. pyogenes* are non-motile spherical bacteria with a diameter of 0.5-1μm (26). Phylogenetically, Gram-positive cocci and spirochetes are also contained in different major lineages (kingdoms) of bacteria. Although the precise role/s of Fn-binding in infection has yet to be demonstrated for bacterial pathogens the identification of a conserved mechanism of Fn binding between streptococci, staphylococci and spirochetes hints at the importance of this mechanism for the bacteria and that it may be more widespread in bacterial/Fn interactions than has been demonstrated to date.

**Acknowledgements**

JRP acknowledges the support of the British Heart Foundation. This work was also supported by the BBSRC and a FEBS Fellowship to SR.

**References**


1. Smith, R., O'Connell, S., and Palmer, S. (2000) *Emerg. Infect. Dis* **6**, 404-407
2. Fraser, C. M., Casjens, S., Huang, W. M., Sutton, G. G., Clayton, R., Lathigra, R., White, O., Ketchum, K. A., Dodson, R., Hickey, E. K., Gwinn, M., Dougherty, B., Tomb, J.-F., Fleischmann, R. D., Richardson, D., Peterson, J., Kerlavage, A. R., Quackenbush, J., Salzberg, S., Hanson, M., van Vugt, R., Palmer, N., Adams, M. D., Gocayne, J., Weidman, J., Utterback, T., Watthey, L., McDonald, L., Artiach, P., Bowman, C., Garland, S., Fujii, C., Cotton, M. D., Horst, K., Roberts, K., Hatch, B., Smith, H. O., and Venter, J. C. (1997) *Nature* **390**, 580-586
3. Grab, D. J., Givens, C., and Kennedy, R. (1998) *Biochimica et Biophysica Acta (BBA) - Molecular Basis of Disease* **1407**, 135-145
4. Schwarz-Linek, U., Hook, M., and Potts, J. R. (2004) *Mol. Microbiol.* **52,** 631-641
5. Joh, H. J., Housepompeo, K., Patti, J. M., Gurusiddappa, S., and Hook, M. (1994) *Biochemistry* **33**, 6086-6092
6. Joh, D., Wann, E. R., Kreikemeyer, B., Speziale, P., and Höök, M. (1999) *Matrix Biol.* **18**, 211-223
7. Molinari, G., Talay, S. R., ValentinWeigand, P., Rohde, M., and Chhatwal, G. S. (1997) *Infect. Immun.* **65**, 1357-1363
8. Jadoun, J., Ozeri, V., Burstein, E., Skutelsky, E., Hanski, E., and Sela, S. (1998) *J. Infect. Dis.* **178**, 147-158
9. Sinha, B., Francois, P. P., Nusse, O., Foti, M., Hartford, O. M., Vaudaux, P., Foster, T. J., Lew, D. P., Herrmann, M., and Krause, K. H. (1999) *Cell. Microbiol.* **1**, 101-117
10. Schwarz-Linek, U., Werner, J.M., Pickford, A.R., Gurusiddappa,S., Kim,J.H., Pilka,E.S., Briggs, J.A.G., Gough,T.S., Höök, M.,Campbell, I.D., Potts, J.R,. (2003) *Nature* **423**, 177-181
11. Schwarz-Linek, U., Pilka, E. S., Pickford, A. R., Kim, J. H., Hook, M., Campbell, I. D., and Potts, J. R. (2004) *J. Biol. Chem.* **279**, 39017-39025
12. Probert, W. S., and Johnson, B. J. B. (1998) *Mol Microbiol* **30**, 1003-1015
13. Fikrig, E., Feng, W., Barthold, S. W., Telford, S. R., and Flavell, R. A. (2000) *J. Immunol.* **164**, 5344-5351
14. Heikkila, T., Huppertz, H. L., Seppala, I., Sillanpaa, H., Saxen, H., and Lahdenne, P. (2003) *J. Infect. Dis.* **187**, 1888-1894
15. Kim, J. H., Singvall, J., Schwarz-Linek, U., Johnson, B. J. B., Potts, J. R., and Hook, M. (2004) *J. Biol. Chem.* **279**, 41706-41714
16. Probert, W. S., Kim, J. H., Höök, M., and Johnson, B. J. B. (2001) *Infect. Immun.* **69**, 4129-4133
17. Talay, S. R., Zock, A., Rohde, M., Molinari, G., Oggioni, M., Pozzi, G., Guzman, C. A., and Chhatwal, G. S. (2000) *Cell. Microbiol.* **2**, 521-535
18. Potts, J. R., Bright, J. R., Bolton, D., Pickford, A. R., and Campbell, I. D. (1999) *Biochemistry* **38**, 8304-8312
19. Soffe, N., Boyd, J., and Leonard, M. (1995) *J. Magn. Reson. Ser. A* **116**, 117-121
20. Johnson, B. A., and Blevins, R. A. (1994) *J. Biomol. NMR* **4**, 603-614
21. Penkett, C. J., Dobson, C. M., Smith, L. J., Bright, J. R., Pickford, A. R., Campbell, I. D., and Potts, J. R. (2000) *Biochemistry* **39**, 2887-2893
22. Williams, M. J., Phan, I., Harvey, T. S., Rostagno, A., Gold, L. I., and Campbell, I. D. (1994) *J. Mol. Biol.* **235**, 1302-1311
23. HousePompeo, K., Xu, Y., Joh, D., Speziale, P., and Höök, M. (1996) *J. Biol. Chem.* **271**, 1379-1384
24. Ingham, K. C., Brew, S., Vaz, D., Sauder, D. N., and McGavin, M. J. (2004) *J. Biol. Chem.* **279**, 42945-42953
25. Ma, Y., Sturrock, A., and Weis, J. J. (1991) *Infect. Immun.* **59**, 671-678
26. Madigan, M., Martinko, J.M., Parker, J. (2000) *Brock Biology of Microrganisms*, 9th Ed., Prentice Hall, Upper Saddle River
27. Thompson, J., Gibson, T., Plewniak, F., Jeanmougin, F., and Higgins, D. (1997) *Nucl. Acids Res.* **25**, 4876-4882
28. Hall, T. (1999) *Nucleic Acids Symposium Series* **41**, 95-98
29. Kraulis, P. J. (1991) *J. Applied Crystallog.* **24**, 946-950
30. Merritt, E. A., and Murphy, M. E. P. (1994) *Acta Crystallographica Section D-Biological Crystallography* **50**, 869-873

**FIG. 1. Sequence alignment of regions of Fn-binding proteins from *B. burgdorferi* (BBK32), *S. pyogenes* (SfbI, SfbII) and *S. aureus* (FnBPA).** Numbers following the hyphens refer to FnBRs as defined previously (4). The N- and C-terminal boundaries of the peptides used in this study are shown above and below the alignment. Predicted binding sites within Fn are shown at the top of the figure. This alignment was chosen to minimise gaps between the predicted F1-binding motifs. If gaps are not minimised, other alignments are possible, for example as shown in Fig.1B. Sequence alignments were performed using the programmes ClustalX (27) and BioEdit (28).

**FIG. 2 The absolute value of chemical shift perturbations of the $^{1}$H and $^{15}$N backbone amide resonances in $^{4}$F1$^{5}$F1 on binding of the BBK32 peptides (A) BBKFF and (B) BBKFo (Fig. 1).** $^{4}$F1$^{5}$F1 concentration was 0.2mM and 0.19mM in A and B, respectively. β-strand secondary structure for the F1 modules is indicated at the top of the figure (A-E for $^{4}$F1 and A'-E' for $^{5}$F1). Residues that could not be traced due to spectral overlap or because they disappear on peptide binding are marked with x. Proline residues are indicated with P. Typical titrations of chemical shift used to calculate the $K_d$ for the interactions of $^{4}$F1$^{5}$F1 with BBKFF and BBKFo are shown in C and D, respectively. The curve is drawn using the $K_d$ calculated from the titration of 16 and 11, respectively $^{15}$N or $^{1}$H chemical shifts of the backbone amides of $^{4}$F1$^{5}$F1 residues. Chemical shift changes are normalised to 1 at saturation.

**FIG. 3 The absolute value of chemical shift perturbations of the $^{1}$H and $^{15}$N backbone amide resonances in $^{2}$F1$^{3}$F1 on binding of the BBK32 peptides (Fig. 1) (A) BBKTT and (B) BBKTw, (C) BBKTTb.** $^{2}$F1$^{3}$F1 concentration was 0.2mM, 0.19mM and 0.06mM in A, B and C, respectively. β-strand secondary structure for the F1 modules is indicated at the top of the figure (A-E for $^{2}$F1 and A'-E' for $^{3}$F1). Residues that could not be traced due to spectral overlap or because they disappear on peptide binding are marked with x. Proline residues are indicated with P. D,E. Titrations of chemical shift perturbation (Δδ) used to calculate the $K_d$ for the interaction of $^{2}$F1$^{3}$F1 with BBKTw (E) and BBKTTb (F). Residue numbers and whether the $^{1}$H or $^{15}$N shift was used are indicated. The curves are drawn using the $K_d$ calculated from at least 8 chemical shift perturbations of the $^{15}$N or $^{1}$H backbone amide resonances of $^{2}$F1$^{3}$F1. Chemical shift perturbations are normalised to 1 at saturation. F. ITC profile for the interaction of BBKTTb with $^{2}$F1$^{3}$F1. *Top*, heat differences obtained for 37 injections. *Bottom*, integrated curve with experimental points (□) and the best fit (—). Data were fitted using a one-site model, resulting in the following: stoichiometry, N=0.985 ± 0.002; $K_d$ = 30 ± 0.4μM; ΔH = -8252 ± 23.8 cal mol$^{-1}$; ΔS = -6.99 cal mol$^{-1}$ K$^{-1}$. FnBR/NTD interactions are ionic-strength dependent; they are weaker on addition of salt (unpublished data). However, to facilitate the ITC experiment, binding is measured in the presence of 10mM phosphate buffer.

**Fig. 4. Chemical shift changes observed in $^{2}$F1 (A-C) and $^{4}$F1 (D-F) on binding of FnBP peptides from *B. burgdorferi* (BBK32), *S. aureus* (FnBPA) and *S. pyogenes* (SfbI).** A. BBKTw B. AuTw1 C. PyTw5 (11) D. BBKFo E. AuFo3 F. PyFo5 (11) $^{1}$H and $^{15}$N chemical shift perturbations are shown in grey and white, respectively. For the BBK32 peptides (A, D), chemical shift perturbations > 0.1ppm and > 0.5ppm, for $^{1}$H and $^{15}$N respectively are shown in red. These highlighted residues are also highlighted in the lower panels (B,C and E ,F) if the chemical shift perturbation is in the same direction. Residues undergoing the largest ($^{1}$H > 0.2ppm and/or $^{15}$N > 1ppm) chemical shift perturbations on addition of BBKTw and BBKFo are mapped onto the structure of $^{2}$F1 ($^{1}$F1$^{2}$F1, PDB accession code 1qgb) and $^{4}$F1 ($^{4}$F1$^{5}$F1, PDB accession code 1fbr), respectively. Residues which could not be traced are shown in grey and all other residues (including proline residues) are shown in cyan. The location of the β-strands is indicated. The figure was drawn using Molscript2 (29) and Raster3D (30).

**Fig. 5 Schematic showing the arrangement of Fn binding sites in SfbI from *S. pyogenes* and BBK32 from *B. burgdorferi*.** To indicate the relative dimensions of the bacteria, the vertical bars next to the pictures represent 1μm. The schematics of the protein molecules are not drawn to this scale. The NTD/NTD-binding sites are shown in dark grey, and the GBD/GBD-binding sites are shown in light grey. The location of the RGD integrin-binding sequence in the $^{10}$F3 module of Fn is indicated.

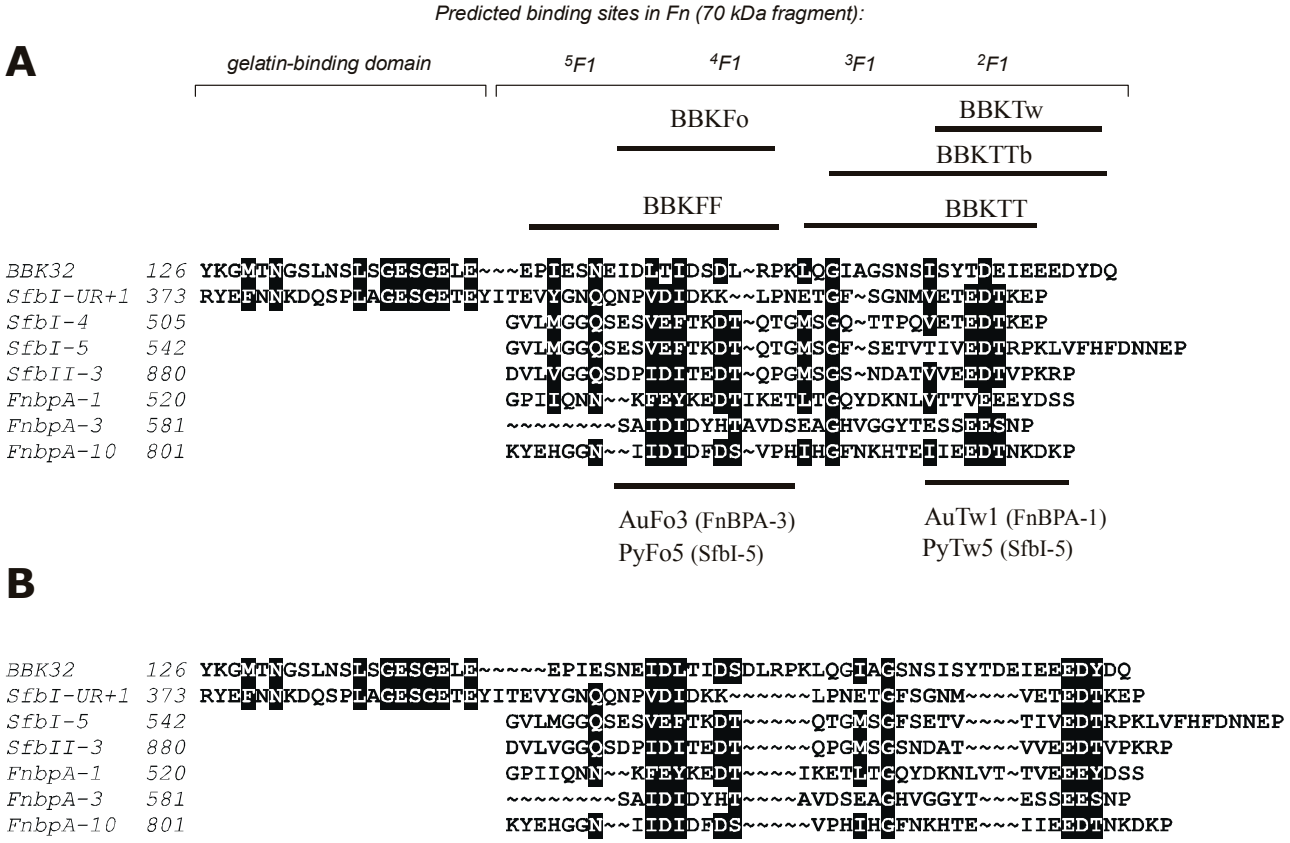
Predicted binding sites in Fn (70 kDa fragment):
A
gelatin-binding domain
5F1
4F1
3F1
2F1
BBKFo
BBKTw
BBKTTb
BBKFF
BBKTT
BBK32 126 YKGMTNGSLNSLSGESGELE~~~EPIESNEIDLTIDSDL~RPKLQGIAGSNSISYTDEIEEEDYDQ
SfbI-UR+1 373 RYEFNNKDQSPLAGESGETEYITEVYGNQQNPVDIDKK~~LPNETGF~SGNMVETEDTKEP
SfbI-4 505 GVLMGGQSESVEFTKDT~QTGMSGQ~TTPQVETEDTKEP
SfbI-5 542 GVLMGGQSESVEFTKDT~QTGMSGF~SETVTIVEDTRPKLVFHFDNNEP
SfbII-3 880 DVLVGGQSDPIDITEDT~QPGMSGS~NDATVVEEDTVPKRP
FnbpA-1 520 GPIIQNN~~KFEYKEDTIKETLTGQYDKNLVTTVEEEYDSS
FnbpA-3 581 ~~~~~~~~SAIDIDYHTAVDSEAGHVGGYTESSEESNP
FnbpA-10 801 KYEHGGN~~IIDIDFDS~VPHIHGFNKHTEIIEEDTNKDKP
AuFo3 (FnBPA-3)
PyFo5 (SfbI-5)
AuTw1 (FnBPA-1)
PyTw5 (SfbI-5)
B
BBK32 126 YKGMTNGSLNSLSGESGELE~~~~~EPIESNEIDLTIDSDLRPKLQGIAGSNSISYTDEIEEEDYDQ
SfbI-UR+1 373 RYEFNNKDQSPLAGESGETEYITEVYGNQQNPVDIDKK~~~~~~LPNETGFSGNM~~~~VETEDTKEP
SfbI-5 542 GVLMGGQSESVEFTKDT~~~~~QTGMSGFSETV~~~~TIVEDTRPKLVFHFDNNEP
SfbII-3 880 DVLVGGQSDPIDITEDT~~~~~QPGMSGSNDAT~~~~VVEEDTVPKRP
FnbpA-1 520 GPIIQNN~~KFEYKEDT~~~~IKETLTGQYDKNLVT~TVEEEYDSS
FnbpA-3 581 ~~~~~~~~SAIDIDYHT~~~~AVDSEAGHVGGYT~~~ESSEESNP
FnbpA-10 801 KYEHGGN~~IIDIDFDS~~~~~VPHIHGFNKHTE~~~IIEEDTNKDKP

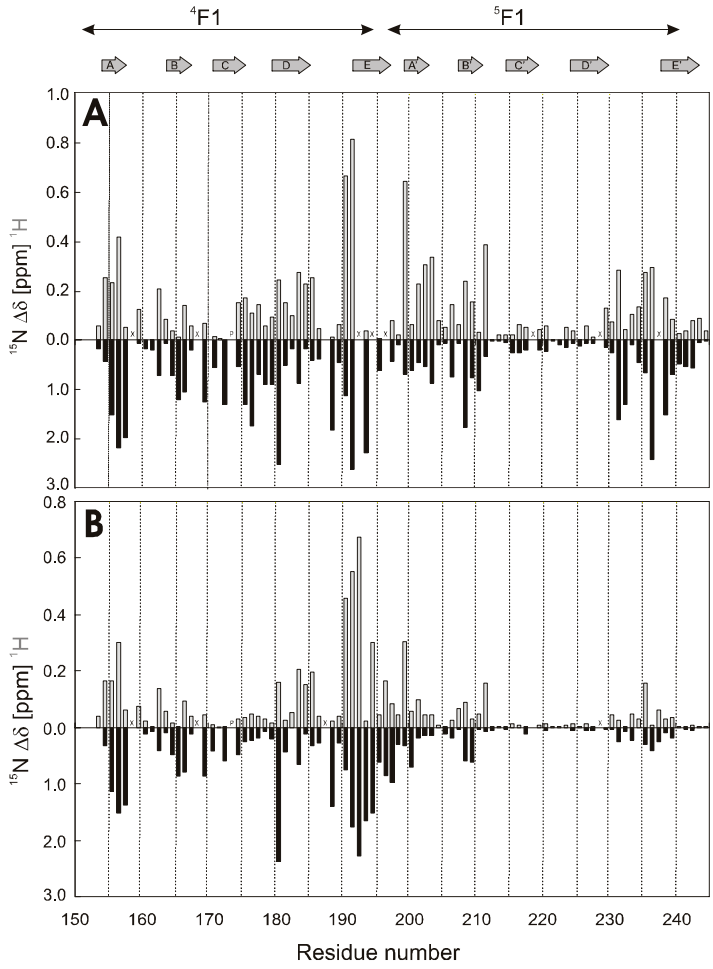
$^4$F1
$^5$F1
A
B
C
D
E
A'
B'
C'
D'
E'
A
B
$^{15}$N Δδ [ppm] $^1$H
Residue number

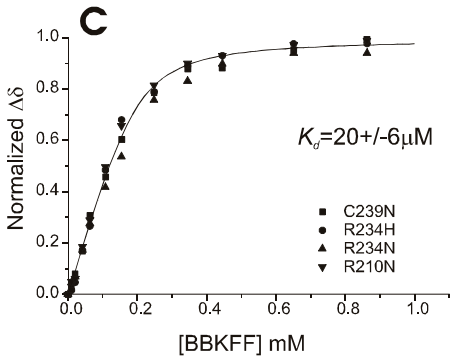
C
Normalized Δδ
$K_d$=20+/-6μM
C239N
R234H
R234N
R210N
[BBKFF] mM

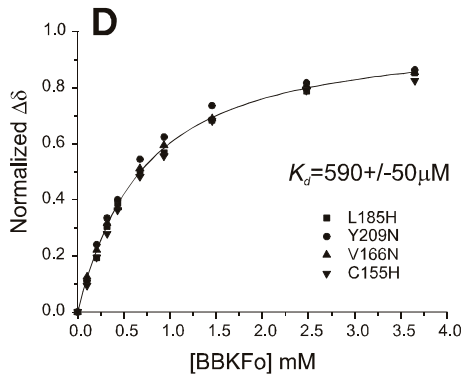
D
Normalized Δδ
$K_d$=590+/-50μM
L185H
Y209N
V166N
C155H
[BBKFo] mM

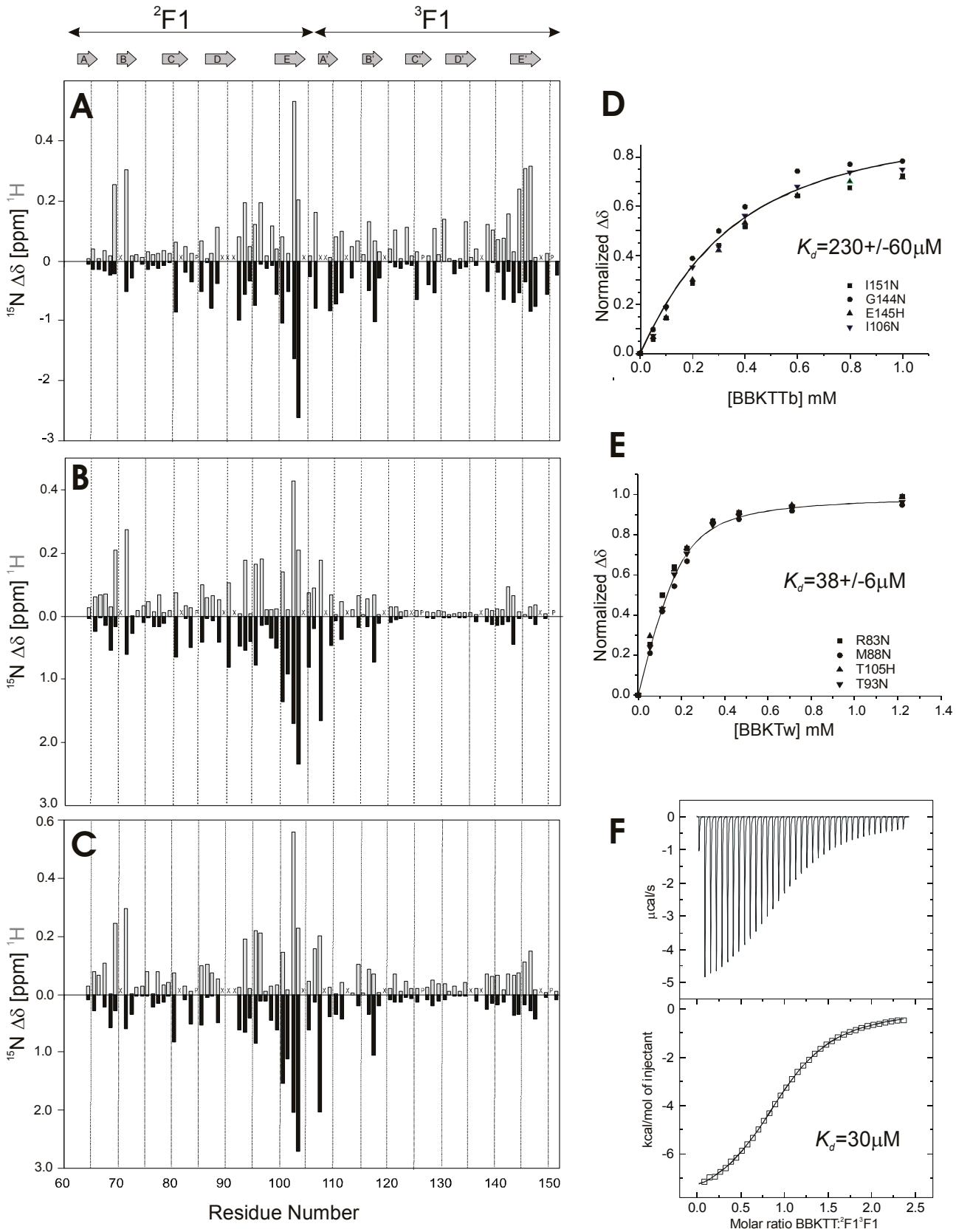
$^2$F1
$^3$F1
A'
B'
C'
D'
E'
A
B
C
D
E
$^{15}$N Δδ [ppm] $^1$H
Residue Number
D
Normalized Δδ
$K_d$=230+/-60μM
I151N
G144N
E145H
I106N
[BBKTTb] mM
E
$K_d$=38+/-6μM
R83N
M88N
T105H
T93N
[BBKTw] mM
F
μcal/s
kcal/mol of injectant
$K_d$=30μM
Molar ratio BBKTT:$^2$F1$^3$F1

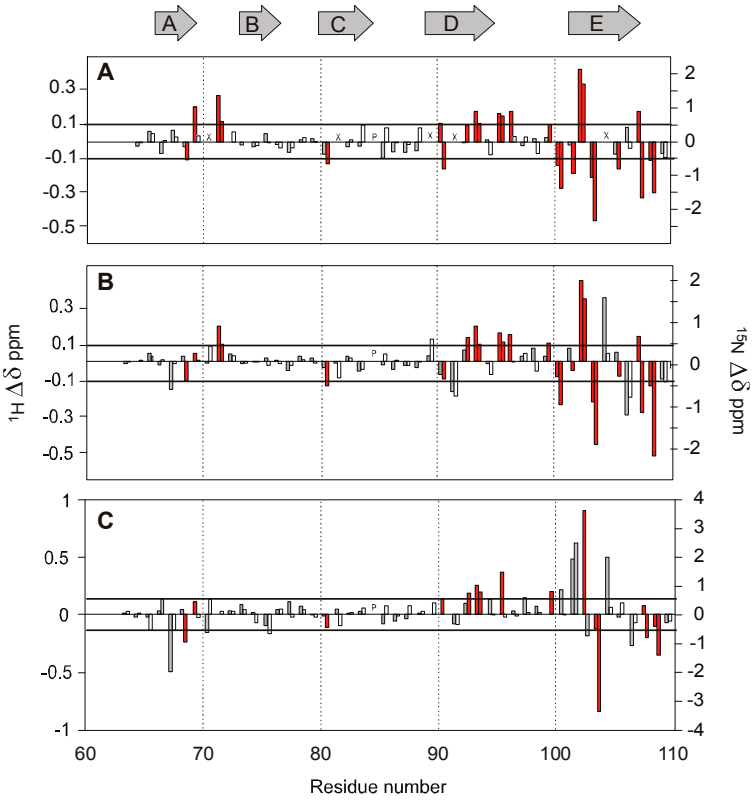
A
B
C
D
E
A
B
C
D
E
0.3
0.1
-0.1
-0.3
-0.5
2
1
0
-1
-2
1
0.5
0
-0.5
-1
4
3
2
1
0
-1
-2
-3
-4
60
70
80
90
100
110
Residue number
$^{1}$H Δδ ppm
$^{15}$N Δδ ppm

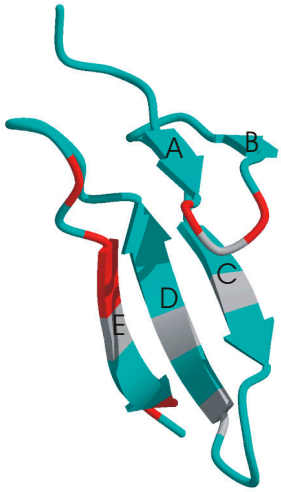
A
B
C
D
E

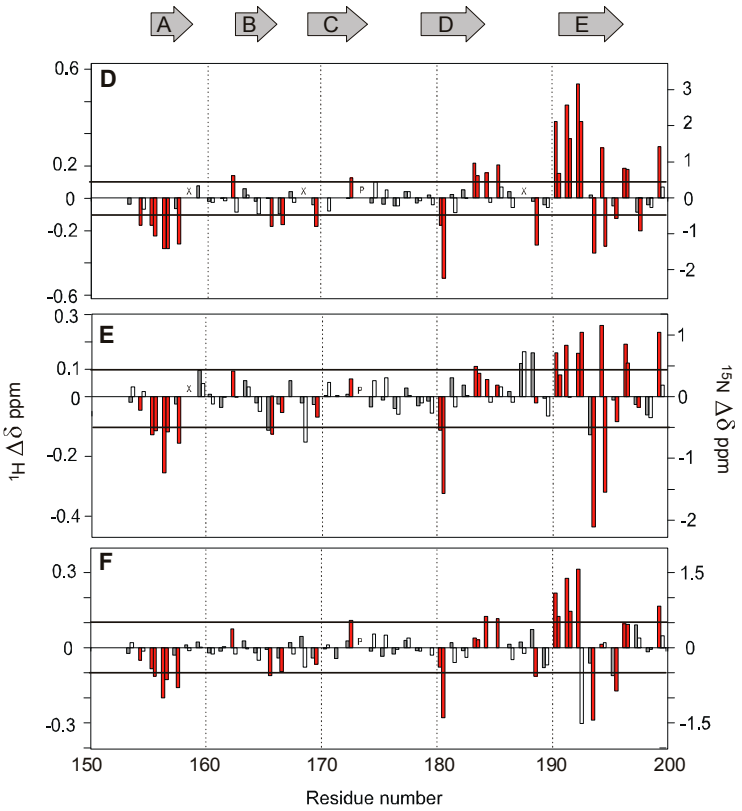
A
B
C
D
E
F
0.6
0.2
0
-0.2
-0.6
0.3
0.1
0
-0.2
-0.4
0.3
0
-0.3
3
2
1
0
-1
-2
1
0
-1
-2
1.5
0
-1.5
150
160
170
180
190
200
Residue number
$^{1}$H Δδ ppm
$^{15}$N Δδ ppm

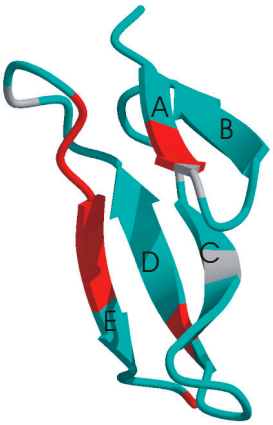
A
B
C
D
E

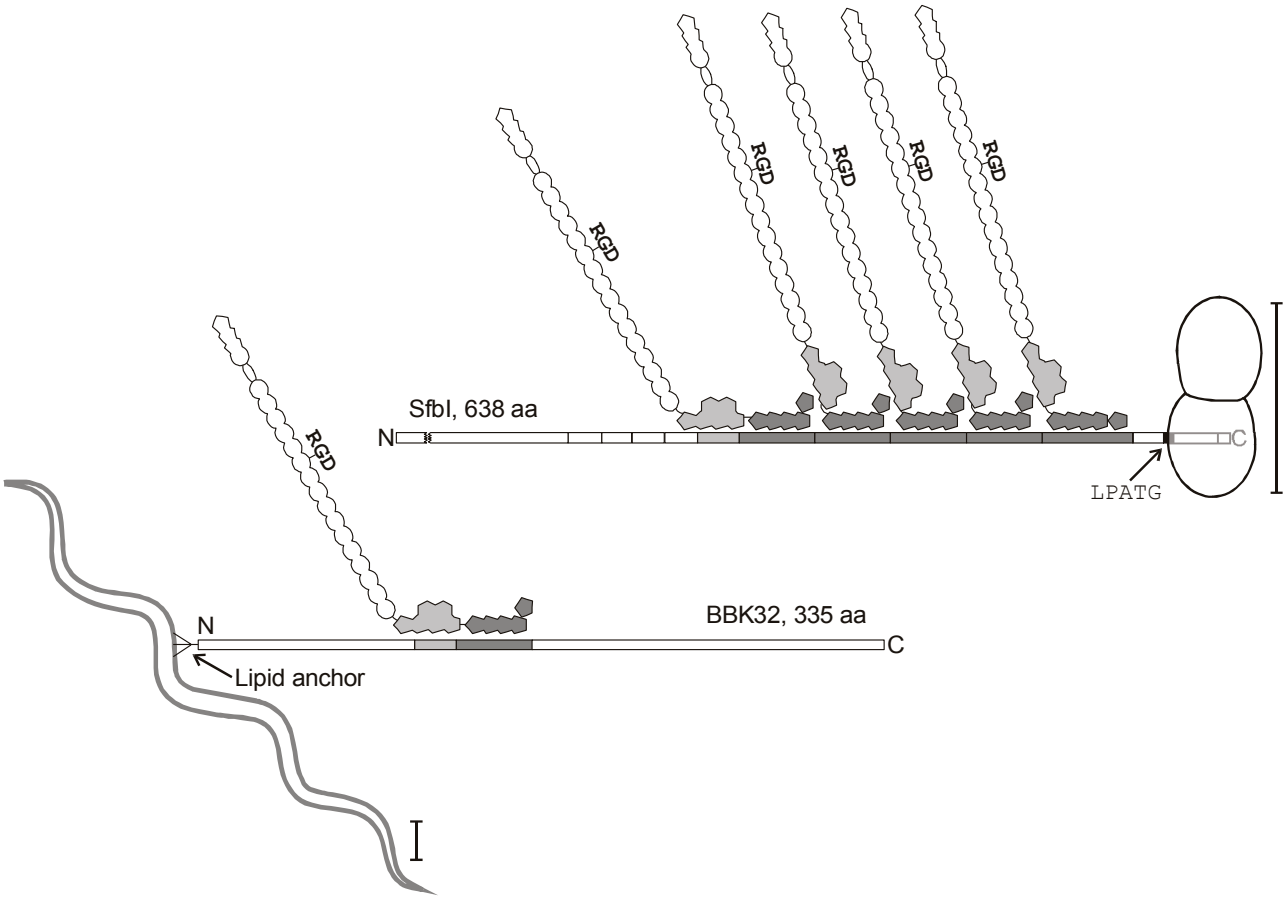
RGD
RGD
RGD
RGD
RGD
RGD
SfbI, 638 aa
N
C
LPATG
N
BBK32, 335 aa
C
Lipid anchor